BUTTERWORTH HEINEMANN

Polymer Vol. 36 No. 9, pp. 1781–1790, 1995

0032-3861/95/$10.00 + 0.00

Low-voltage scanning electron microscopy of polymers*

J. H. Butler†
Exxon Chemical Company, Baytown Polymers Center, PO Box 5200, Baytown, TX 77520, USA

and D. C. Joy
University of Tennessee, EM Facility, F239 Walters Life Sciences Building, Knoxville, TN 37996, USA

and G. F. Bradley
University of Tennessee, Department of Chemistry, Knoxville, TN 37996, USA

and S. J. Krause
Arizona State University, College of Engineering and Applied Sciences, Department of Chemical, Bio and Materials Engineering, Tempe, AZ 85287, USA

Micromorphological and microstructural characterizations of the type and degree of crystallinity and the relative dispersion of phases within polymers, as well as in the study of their surfaces and associated interfaces, offer a number of challenges in the field of materials science of polymers. Microscopy is a natural methodology for the acquisition of microstructural information, but for polymers there are few straightforward techniques. Conventional electron microscopy methods are limited in their ability to address fine surface details or to determine the bulk microstructure of multicomponent polymeric materials. Sometimes these problems can be overcome, but only within the practical restrictions associated with meticulous sample preparation.

An extremely promising and efficient alternative to conventional approaches is the state-of-the-art, low-voltage scanning electron microscope (LVSEM). It is demonstrated here that straightforward operation of anLVSEM equipped with a field emission gun (FEG) source can produce topographical contrast secondary electron images of polymers at substantially higher magnifications than a conventional SEM, and with a resolution that rivals TEM. An added advantage is the capability of being able to produce contrast based on differences in chemical composition within the sample. The ability to produce quality images at low accelerating beam voltages minimizes beam damage to the sample, and affords an operating window (e.g. E_2) where the sample does not build up negative charge. This obviates the normal requirement to coat samples with a conductive layer.

We also describe experimental and theoretical developments that can help us to understand the physics of interaction between low-voltage electron beams and polymer samples. This knowledge base, along with further theoretical and instrumental development and the subsequent applications to polymers, promises a whole new field of electron microscope methodology based on the LVSEM.

(Keywords: low-voltage SEM; field emission; microstructure)

INTRODUCTION

Polymers are notorious for the resistance they offer to microscopic examination. Hence the micromorphological and microstructural characterization of the relative dispersion, the type and degree of crystallinity, and the degree of crystalline continuity of different phases within polymeric alloys, blends and composites, as well as the study of polymer surfaces and interfaces, remain challenges for today's materials scientists. Few straightforward techniques can be employed to produce contrast in conventional electron microscopes; consequently they are limited in their ability to address fine surface details or to determine the bulk microstructure of multicomponent polymeric materials. Sometimes this problem can be overcome, but only within the practical restrictions associated with meticulous sample preparation (chemical extraction of phases, oxidative staining, etc.). Polymers are also generally susceptible to beam-induced radiation damage and, as non-conductors, they charge heavily under the scanning electron microscope (SEM) beam. The charging may be overcome and image resolution

* Presented at 'Aspects of Imaging in Polymer Science', 51st Annual Meeting of the Microscopy Society of America, 1–6 August 1993, Cincinnati, OH, USA

† To whom correspondence should be addressed

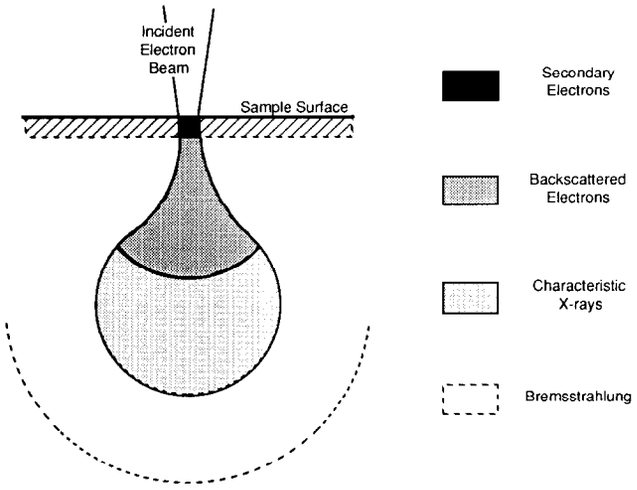

Figure 1 Beam–sample interaction volume for conventional SEM. Generalized illustration of interaction (i.e. signal source) volumes for various electron–specimen interactions. Electron-excited X-rays emerge from deepest within the sample and have the poorest resolution

increased with the use of a transmission electron microscope (TEM), but this increases the potential for beam damage and forces large amounts of laboratory resources to be concentrated on the generation of undeformed, ultrathin samples. Also, the TEM ability to image surface morphology is minimal without equally demanding sample preparation (i.e. replication) efforts.

An extremely efficient alternative for the analysis of polymers is the state-of-the-art, field emission gun (FEG) source, high-resolution, low-voltage scanning electron microscope (LVSEM). LVSEMs minimize the above-mentioned problems, while they rival TEMs for image resolution. The high brightness produced by the FEG allows the electron probe to be focused down to nanometre dimensions yet still retain enough intensity to produce usable signal levels. Furthermore, the high probe intensity produces acceptable signal intensities at very low accelerating voltages (nominally 1–2 kV). This affords three major advantages: (1) higher resolution, (2) negligible beam damage of samples and (3) absence of the need for coating samples with conducting films to eliminate sample charging under the beam. The latter is a double advantage for a high-resolution instrument because at high magnifications one wants information about the 'neat' surface, not the detailed morphology of the coating.

CONVENTIONAL SHORTCOMINGS

Resolution and contrast

Figure 1 schematically illustrates SEM beam–sample interaction volumes at conventional accelerating voltages. The actual size and shape of the interaction 'teardrop' depends on the sample composition as well as incident beam energy; and the intensity ratios for the various types of signal generated at different incident beam energies are quite different[1]. In a carbonaceous material the secondary electrons ($E \leqslant 50$ eV) escape from a depth of $\leqslant 20$ nm regardless of the incident beam energy. Thus the only way to improve secondary electron image (SEI) resolution is to use an accelerating voltage, E_0, so low that the interaction volume dimensions are less than this 20 nm escape depth. This effect is prominent when features of interest in the surface topography are of the same (or smaller) size as the interaction volume; in this situation surface features can be 'washed out' because of beam penetration through the structure[2].

Of course, the main reason that the new LVSEMs can form images with high resolution is simply that, owing to their field emission electron optics, they can produce extremely finely focused (≈ 2.5 nm) probes at very low (1–2 keV) beam energies and can do even better (< 1.0 nm) at higher (> 10 keV) beam energies.

The differences in secondary electron emission from different phases within multicomponent materials depend on a combination of factors such as the nature of the molecular bonds, the elements present, amorphous/crystalline nature of each phase, conductivity, work function, etc. Since the secondary electron yield for all materials increases as incident beam energy decreases, it should be possible to produce SEI contrast as a result of compositional differences in the sample. This has been illustrated for the case of various polymer blends[3]. The great advantage here, of course, is elimination of the need for heavy-atom staining or chemical extraction in order to generate compositional contrast in SEIs of these materials. Mismatch in properties such as viscosity, ductility, hardness/softness, etc., of various components shows up as topographical contrast (the only type of contrast available at conventional SEM voltages).

Charging of samples

One of the biggest problems with SEM of polymers at conventional voltages is their great propensity to accumulate negative charge and consequently to reject the incident probe in successive scans. Obviously this situation exists because the electrons that impinge on the sample surface do not drain away faster than they are supplied by an intense, high-energy probe. The physical attribute of conductivity allows accumulated charge to be dispersed in the case of metal and some semiconductor samples, but is not an advantage enjoyed by polymers and other non-conductors. However, conductivity is not the only way that materials disperse accumulated charge from an incident probe: they also emit secondary (SE) and backscattered (BS) electrons. At very low accelerating voltages the fact that the SE escape depth is of the same order as the incident electron penetration depth can be used to eliminate the build-up of surface electron charge. At some given accelerating beam energy, E_2 (or E2), the sum of the secondary and the backscattered currents equals that of the incident beam. Under these conditions charge is neither injected into nor extracted from the sample, and it is theoretically possible to image non-conducting materials without coating them with metal.

The first defence against sample charging is to tilt the sample at a high angle relative to the beam. This provides a more favourable geometry for the escape of secondaries from the sample surface. Further along these lines, it will be shown later that samples with fine surface micro-textures (i.e. roughness on the scale of a few nanometres) do not charge nearly as quickly as samples with roughness variations on a larger scale.

There are several other possible solutions to the specimen charging problem (cf. *Table 1*). One method is to use faster scan speeds so that the dwell time of the

Table 1 Reducing negative sample charging

Lower accelerating voltage
Lower beam current
Faster scan speed with an integrating frame buffer
High sample tilt
Thin (≈ 1 nm) metal sputter-coated films
Use BS imaging instead of SE imaging
Microtexture of specimen

beam on each microvolume of the sample is minimized. This approach increases the amount of (speckle) noise in any single image, but when an integrating frame buffer is used to collect and average several frames, the noise disappears. Another solution employs new ion beam (Magnetron) sputter coating technology to deposit a <2 nm uniformly thin coating of amorphous Cr, enough to drain off the accumulated charge yet thin enough not to obscure surface details of nanometre dimensions.

Final alternatives to low-voltage sample charging employ backscattered (BS) electrons. Since the BS electrons escape with a much higher energy than the SEs, the contribution to the SEIs from charging can be 'tuned' out simply by biasing the specimen[4]. Also, new backscattered detector technologies that can produce usable signal levels even at very low incident beam energies are emerging[5].

Beam-induced sample damage

Since the vast majority of the energy in the incident electron probe is lost by conversion into heat at the irradiation point, conventional accelerating voltages may cause deterioration, decomposition, sublimation, deformation and cracking of the sample. At the accelerating voltages available with LVSEM, sample damage is less than at conventional SEM voltages. Although not well quantified for polymers, sample damage becomes appreciably small at 2 keV and below. Thus one can increase the overall electron dose to several hundred times that which is used at conventional voltages.

DEVELOPMENTS

Electron beam–sample interaction

In order to reap the maximum benefits of the LVSEM high-resolution capabilities, it is essential to develop methods for obtaining and interpreting images of uncoated polymers. This is necessary because the conductive coating (nominally ≈ 20 nm thick) that is usually deposited on SEM samples to prevent their charging under the beam obscures the features of interest (nominally 3–50 nm in size). Also, residual charge build-up can cause damage and distortion of detailed features. At conventional SEM beam energies there is no way to circumvent this problem; but at the very low incident beam energies available in the LVSEM the secondary electron yield increases, and it is possible to reach an imaging situation where zero net charge resides on the sample surface. The conditions under which this situation occurs for any given sample are a function of the sample's chemical composition, density, dielectric properties and surface roughness, as well as the incident beam energy.

Obviously the beam energy, E_2, at which charge balance occurs is of key interest. Consequently our initial goal has been to investigate electron-beam-induced charging and to try to associate the parameters that we measure with physical and chemical properties of different polymers. The first stage has been to build a database of E_2 values from a number of polymeric materials. E_2 can be determined experimentally as well as theoretically, and developing proper models to bring experimental and theoretical values into coincidence provides a wealth of knowledge about the physical properties of the sample.

Electron emission in the LVSEM

Whenever an electron beam of energy E_0 irradiates matter, various types of electrons (secondaries, backscattered, Auger, etc.) are emitted from the surface of the target. According to their energy, E, the electrons can be classified as belonging to one of two groups: (1) $E < 50$ eV, secondary electrons; and (2) $50\text{ eV} < E < E_0$, backscattered (reflected) electrons[6].

If we define the *secondary electron yield*, δ, as the number of (inelastically scattered) secondary electrons ($E < 50$ eV) emitted per incident electron and, analogously, the *backscattered electron yield*, η, as the number of (elastically) backscattered electrons ($E > 50$ eV) emitted per incident electron, then (since Kirchhoff's law must apply to this situation) we have the condition:

$$I_B = \delta I_B + \eta I_B + I_{SC} \quad (1)$$

where I_B is the beam current, and I_{SC} is the current flowing to or from earth to the specimen. If the specimen is not an electrical conductor then I_{SC} is zero and consequently a charge imbalance is generated in the sample of magnitude:

$$I_B[1-(\delta+\eta)] \quad (2)$$

For a polymer irradiated with a beam energy of a few keV, $(\delta+\eta)$ is less than unity; thus the charge accumulates in the sample, which therefore acquires a negative potential. Since the electron source is negative with respect to ground the effective potential energy of the beam is reduced. Both δ and η are functions of the beam energy and, typically for a polymer, their magnitude increases with a decrease in incident beam energy as illustrated in *Figure 2*.

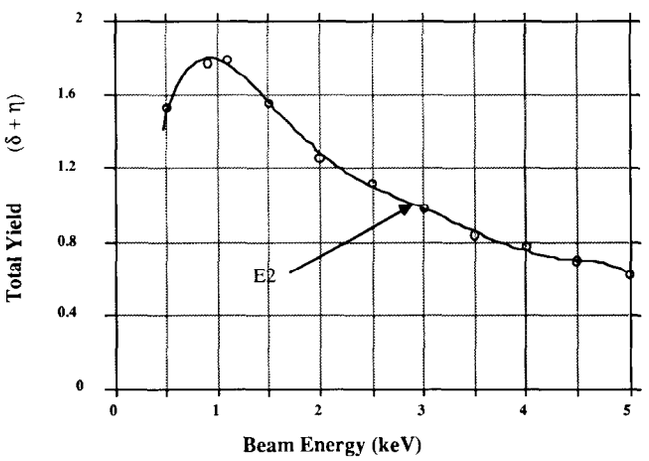

Figure 2 Total yield $(\delta+\eta)$ for carbon as a function of incident beam energy, E_0

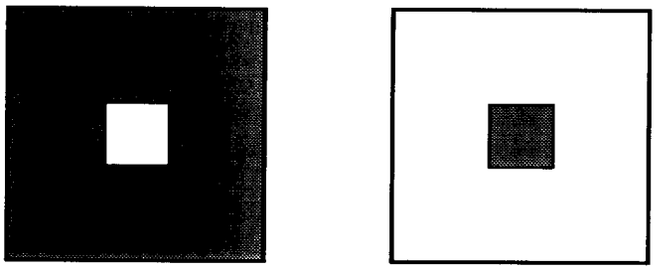

Figure 3 Sample charging when $E_0 > E_2$ and $E_0 < E_2$

If the initial incident energy is high enough so that $(\delta + \eta)$ is less than unity, then under constant irradiation the sample will continue to charge negatively until the effective landing energy of the electrons is such that $(\delta + \eta)$ is equal to unity. At this energy, usually referred to as E_2, the sample is in a dynamic charge balance condition. If the initial energy is below E_2 then the sample will charge positively and re-collect secondary electrons until once again the effective incident energy becomes E_2.

E_2 is clearly the single most important parameter describing the charge-up behaviour of a polymer and consequently our initial work has been aimed at obtaining values of E_2 for a wide range of polymers. Secondly, we wish to see how E_2 correlates with other properties of the polymer such as composition, density and surface condition, with the final goal of being able to predict E_2 purely on the basis of chemical and physical data. Ultimately we wish to be able to identify uniquely among polymers of different types within the LVSEM operating at various E_2 values.

Experimental determination of E_2

There are two basic experimental methods to determine the value of E_2:

(i) *The imaging technique.* This is the quickest and easiest method. The procedure is to select an accelerating voltage, and observe the SE image of the sample at a low magnification ($\times 20$ $\times 50$). Then switch to a high magnification ($\times 500$– $\times 2000$) for a few seconds before dropping back to the original low magnification.

As illustrated in *Figure 3* if the afterglow of the high-magnification scan square is bright, then that region was charging negatively and the beam energy is above E_2; while if the small scan square is dark, then the sample is charging positively and E_0 is below E_2. The exact value of E_2 can typically be bracketed to ± 50 eV within a few minutes in this manner.

(ii) *Capacitance method*[7]. In this approach the electron beam is used as a virtual electrode and the sample is then the dielectric in a parallel-plate capacitor. At time $t = 0$ the beam of energy E_0 is allowed to scan an area, previously unexposed, of known size on the specimen while monitoring the electrostatic potential on the sample with an electrometer using a strip chart recorder or a computer. The experimental arrangement is illustrated in *Figure 4*.

If the measured specimen current is I_B and the potential at some time, t, is $V(t)$, then:

$$V(t) = \frac{1}{C}\int_0^t I_B \, dt \tag{3}$$

where C is the effective capacitance of the sampled area. When $E_0 > E_2$ then $(\delta + \eta) < 1$, the specimen current and hence $V(t)$ are negative; while if $E_0 < E_2$ then $V(t)$ is positive. Hence E_2 can again be determined. A benefit of this approach is that it also provides information about the dynamic charge-up behaviour of the sample. For example, *Figure 5* plots the saturation (i.e. $t \to \infty$) value of $V(t)$ for a sample of SiO_2/Si glass as a function of incident beam energy.

Actually, there are two ways of making this capacitance measurement. The first, so-called 'static', method (developed for polymers by Vaz and Krause[8]) exposes the sample to the beam and then measures the potential after the beam is turned off. An extension of this method measures the potential while the sample is still being irradiated, and is hence termed the 'dynamic' method. It is therefore expected that there will be divergences in the magnitude of the measured potential between the two approaches for various beam energies. However, both techniques should provide the same value for E_2. The differences in potential measured by the two methods will depend on the mechanisms by which charge is eliminated within the

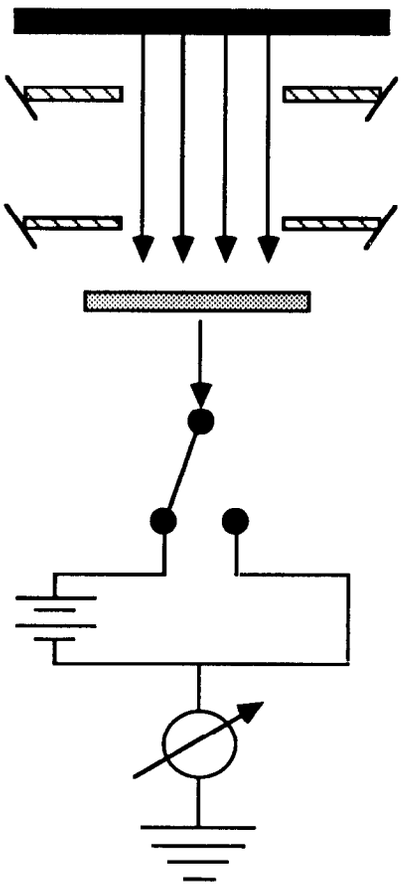

Figure 4 Experimental arrangement for measuring E_2 via the capacitance method. During the experiment the beam is blocked using the condenser aperture. A previously unexposed area is then moved into position and the aperture is opened to expose the specimen to the beam. The current vs. time output is then recorded with a Keithley electrometer

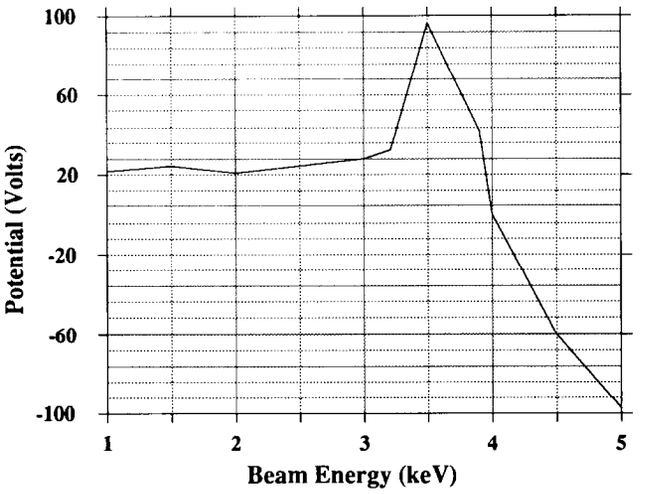

Figure 5 Capacitance method measurement of surface potential vs. E_0 for a silicate glass

solid once irradiation ceases. By employing both methods on the same sample, differences between the two measured potentials can provide information as to the nature of charge storage and dissipation within a polymer (which might even be correlated with macroscopic electrical properties such as dielectric constant and conductivity).

The E_2 energy is clearly defined as that at which the surface remains uncharged. It is, however, obvious from *Figure 6* that the description given above of charging dynamics is an oversimplification since the surface is capable of maintaining a positive or negative potential during irradiation, i.e. it does not float to E_2 as predicted. Our aim is to employ dynamic measurements of this type on polymer samples to see whether this behaviour is typical of all insulators or is material-dependent. Based on these results a more detailed model of the charge-up can then be formulated.

THEORETICAL ASPECTS

Theory of secondary electron emission (SEE)

If the processes of secondary and backscattered electron emission from a polymer can be modelled in enough detail then the value of E_2, as well as of other parameters of interest, could be computed. Since η is typically 10 times less than δ, essentially all theories proposed so far ignore the direct contribution of backscattered electrons to the total emission current.

Secondary electron emission is a complex phenomenon that involves:

(i) SE production via interactions between energetic electrons and a solid—the four basic types are summarized in *Table 2*;

(ii) secondary electron transport to the sample surface; and

(iii) emission of secondaries over the surface potential barrier—electrons of different E have different escape depths.

Because of these three considerations for beam–sample interaction, a number of physical parameters (cf. *Table 3*) can affect secondary electron production, absorption and detection (i.e. the experimental 'yield').

Even though core electron excitation and phonon excitation contributions can be ignored at low voltages, the task of deterministically modelling secondary electron emission is monumental. Thus the traditional methods are all empirical (or at least semi-empirical) in nature. According to *Table 3*, our experiment is less complicated if we are consistent in our experimental arrangement (i.e. always use the same tilt, etc.) as well as in our sample preparation (i.e. consistent surface smoothness). We also ignore work-function effects (for secondaries) as well as conductivity (for polymers). Thus our formulation will adopt a semi-empirical approach, which only considers

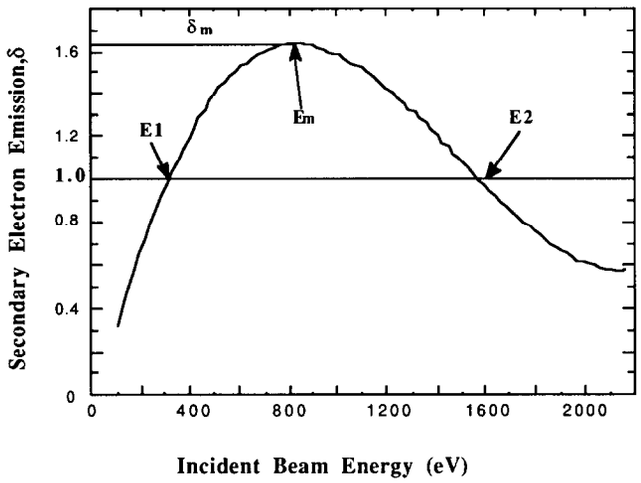

Figure 6 'Universal' yield curve for secondary electron emission (SEE)

Table 2 The four basic types of interactions between energetic electrons and solids

Core electron excitation	This is ionization by excitation over the Fermi level; E_0 must be sufficiently high for this to occur
Valence excitation of single electrons	This corresponds to interband and intraband quantum state transitions and typically produces secondary electrons with $E \approx 3$–20 eV
Plasmon excitations	These are collective excitations of valence electrons via energy coupling to the volume plasma oscillation of the electron gas within a solid
Phonon excitations	This is the excitation of surface vibrations; typically the SE emission energy, $E \approx 100$ meV, is too small to be measured

Table 3 Physical parameters that affect secondary yield

Constituent elements
Nature of molecular bonds
Amorphous vs. crystalline nature
Density
Conductivity
Surface work function (relatively unimportant)
Sample tilt relative to beam
Surface roughness ('microtexturing')

the sample's constituent elements, the molecular bonds and the density.

The simple 'generic' model for secondary emission was proposed originally by Salow[9], independently in a modified form by Bethe[10], and developed by Dekker[11] among others. If we take $N_{SE}(S,E)$, our 'secondary yield rate', as the number of secondary electrons produced at a distance S (measured along the electron trajectory) within the sample, and $p(S)$ as the probability of a secondary electron generated at a depth S escaping to the surface and being detected, then we can write an expression for secondary electron production as simply the integrated product of the yield rate and the escape probability:

$$\delta = \int_0^R N(S,E)p(S)\,dS \tag{4}$$

where R is the 'range' or penetration depth of the electron into the sample.

The Dekker model makes two basic assumptions:

(i) The rate of secondary electron production is proportional to the instantaneous stopping power of the incident electron with energy E:

$$N_{SE} = -\frac{1}{\varepsilon}\left(\frac{dE}{dS}\right) \tag{5}$$

where ε is the average energy required to generate a secondary electron.

(ii) The probability of a secondary electron generated at a depth S beneath the surface escaping to the surface and being collected is:

$$p(S) = 0.5\exp(-S/\lambda) \tag{6}$$

where λ is the average mean free path length.

The integrated value for secondary electron production is then:

$$\delta = -\frac{0.5}{\varepsilon}\int_0^R \left(\frac{dE}{dS}\right)\exp\left(-\frac{S}{\lambda}\right)dS \tag{7}$$

Now we make two simplifying assumptions: assume the electron to travel in a straight line (i.e. ignore backscattering), and assume the instantaneous stopping power is constant and equal to the incident energy divided by the range:

$$dE/dS = E/R \tag{8}$$

Then we have a closed expression for secondary electron production,

$$\delta = \frac{0.5E\lambda}{\varepsilon R}\left[1-\exp\left(-\frac{R}{\lambda}\right)\right] \tag{9}$$

The purpose of the two simplifying assumptions is to remove the necessity to know the value of ε and λ. It is readily shown that the maximum secondary yield δ_m occurs when the beam range is about 2.3λ. If the energy at which the yield reaches the maximum δ_m is E_m then a 'universal' yield curve expression can be derived from (9), which contains only the quantities E, E_m, δ and δ_m:

$$\left(\frac{\delta}{\delta_m}\right) = 1.11\left(\frac{E}{E_m}\right)^{-0.35}\left\{1-\exp\left[-2.3\left(\frac{E}{E_m}\right)^{1.35}\right]\right\} \tag{10}$$

This expression has the general graphical form as shown in *Figure 6* (as well as *Figure 2*).

Semi-empirical model of SEE for polymers

The above 'universal yield' equation (10) can be cast into the form (as can all rate equations):

$$\delta = KE^{-n} \tag{11}$$

By fitting measured values for a number of polymers, Burke[12] was able to obtain:

$$\delta = KE^{-0.725} \tag{12}$$

K can be written any number of ways. One approach Burke[12] took was to equate the asymptotic energy variation of the yield to an empirical expression involving the number of valence electrons, VE, and molecular weight, MW, per monomeric unit:

$$K = 10.64(VE/MW) - 3.15 \tag{13}$$

Using this quantity together with values of δ_m and E_m derived from a variety of measurements, Burke's formula can then be used to compute E_2 values from a wide range of polymers. Alternative formulations due to Burke put

$$K = 1.273\delta_m E_m^{0.725} \tag{14}$$

and

$$K = 12.09E_m^{1.725} \tag{15}$$

Table 4 lists our measured E_2 values in keV for many commercially available polymers. The values range from a minimum of 0.9 to a maximum of 1.6 keV. All the values were taken at room temperature and are the averaged result of four independent 'scan-square' method measurements. *Figure 7* plots these data points as a function of the ratio (VE/MW) of the constituent monomeric units.

Equations (13), (14) and (15) do not always give identical values for E_2 since they are based on different subsets of Burke's data. *Table 4* and *Figure 8* therefore show both estimates for comparative purposes, identifying them as E_2 (using equations (12) and (13)) or (*) (using equations (12) and (14) or (15)).

Figure 8 shows that Burke's equations produce values for E_2 which, when plotted against the ratio (VE/MW), define a lower bound for the experimental data. Although the two variants of the equation produce somewhat different estimates for E_2, both usually lie on the low side of the experimental data. While it cannot be claimed that Burke's equations have any predictive value, they do at least suggest that the quantity (VE/MW) is a significant index for E_2. Since the model involved is a very simplistic one, it is probable that a more detailed analysis might yield a more useful relation. For example, recent work by Kishimoto *et al.*[13] suggests that the π-electron fraction (i.e. the ratio of π-bonds to σ-bonds in the monomeric unit) also appears to be a meaningful index.

Future development of semi-empirical model of SEE

The E_2 values produced in *Table 4* are sensible, but the overall accuracy of the predicted yield curve is poor when compared to the experimental data. Possible reasons for this are:

(i) The Dekker model ignores the effect of scattering in general and backscattering in particular. At low beam energies (<2 keV) a high fraction (as much as 30%) of the secondary electrons are produced by backscattered electrons, and, consequently, failing to include this term leads to a systematic error. At high energies the effect of

Table 4 Experimental and theoretical second crossover energies (E_2) in keV

Polymer[a]	Measured E_2	Burke (*)	Burke's E_2	*VE*	*MW*
Polysulfone 3703	1.1	0.70	0.61	160	442
PBT Celenex 2002	1.1	0.88	0.84	83	219
ABS 901 Magnum	1.1	0.98	0.98	82	211
HIPS Styron	1.3	0.92	0.94	40	104
Nylon-6	1.2	1.18	1.13	45	112
PET Traytuf 7200	0.9	0.79	0.72	70	189
Polyethylene 8054 N	1.5	1.41	1.61	18	42
ABS	1.3	0.98	0.98	82	211
EVOH	1.4	1.20	1.15	28	70
High-density polyethylene	1.5	1.41	1.61	18	42
Isotactic polypropylene	1.4	1.41	1.61	18	42
Kraton 1107	1.5	1.10	0.91	38	99
Low-density polyethylene	1.5	1.41	1.61	18	42
Poly(ethylene-*co*-vinyl acetate)	1.3	1.03	1.04	44	112
Poly(ethylene-*co*-acrylic acid)	1.2	1.04	1.06	39	99
Poly(butadiol 1,4-terephthalate)	1.5	0.91	0.88	84	220
Polycaprolactone	1.4	1.14	1.20	46	114
Polycarbonate	1.3	0.87	0.83	96	254
Polystyrene	0.9	0.94	0.92	40	104
Poly(styrene–acrylonitrile)	0.9	0.69	0.60	56	155
Poly(ethylene terephthalate)	0.9	0.79	0.72	70	189
Poly(ethylene-*co*-propylene)	1.2	1.23	1.33	28	68
Nylon-6/nylon-6,6 copolymer	1.2	1.16	1.23	137	338
EVOH Soranol D 2908	1.3	1.20	1.15	28	70
PMMA	1.6	1.58	1.87	40	90
Kraton 1901x	1.4	0.93	0.91	38	99

[a] PBT = poly(butylene terephthalate)
ABS = acrylonitrile–butadiene–styrene copolymer
HIPS = high-impact polystyrene
PET = poly(ethylene terephthalate)
EVOH = ethylene–vinyl alcohol copolymer
PMMA = poly(methyl methacrylate)

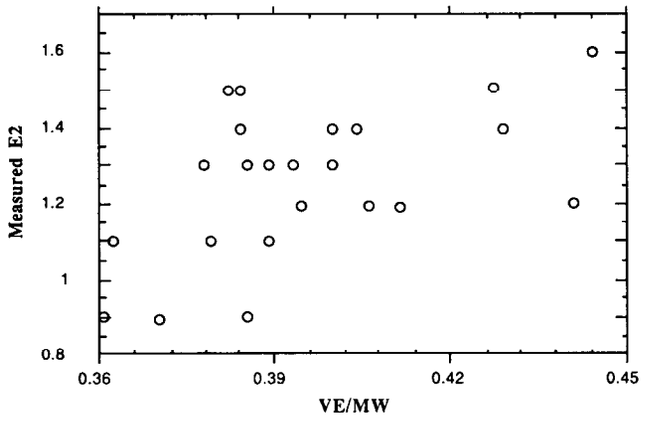

Figure 7 Measured E_2 vs. the ratio of valence electrons to molecular weight

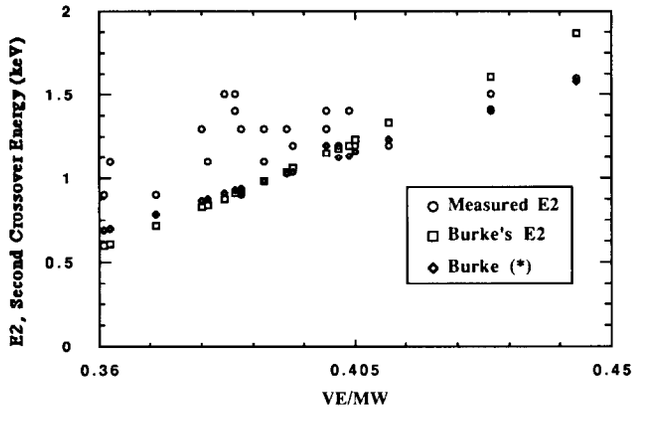

Figure 8 Experimental and theoretical data vs. the ratio of valence electrons to molecular weight

scattering is to bring more incident electrons back towards the surface and again increase the yield compared to a zero-scattering approximation.

(ii) The stopping power approximation invoked in this model is crude and inaccurate especially at low beam energies.

Thus, although this model has the merit of simplicity, the data produced are really of little value for any predictive purposes. However the observations by Burke[12] that E_2 appears to be coupled to the number of valence electrons in the monomer as well as that of Kishimoto *et al.*[13] that there is a functional dependence on the ratio of π- to σ-bonded electrons suggest two significant parameters.

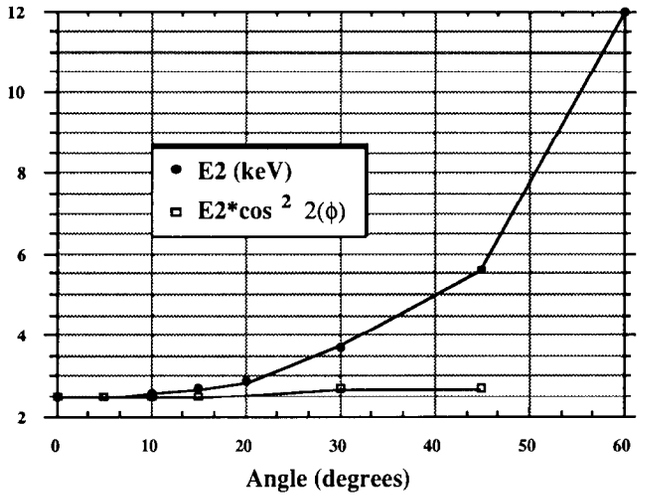

Figure 9 Predicted dependence of E_2 vs. incident beam angle

An improved approach would be to take the essential elements of the Salow–Dekker model but to incorporate them in a Monte Carlo simulation of electron scattering (see Joy[14]). The Monte Carlo model fully accounts for all the scattering and backscattering experienced by an incident electron and also provides a full and accurate expression for the electron stopping power. This approach is therefore capable of predicting the variation of secondary and backscattered yield with incident beam energy with good accuracy provided that appropriate values for ε and λ can be obtained.

A prediction of the Monte Carlo model that has been verified is the variation of E_2 with angle of incidence, ϕ (*Figure 9*). The computed value of E_2 doubles for a 45° angle of incidence and changes of this magnitude are experimentally observed. In fact, for low-atomic-number materials the model predicts that E_2 will vary as approximately $1/\cos^2\phi$, and this is in close agreement with the measurements of Sugiyama *et al.*[15] on glass and with the data of Vaz and Krause[8] on Teflon. It has not been possible so far to suggest a simple analytical explanation for the $1/\cos^2\phi$ variation of E_2 although it is obvious that tilting the sample increases both the secondary and backscattered electron yields by bringing electrons closer to the surface (i.e. reducing the primary penetration depth).

If, however, the surface of the sample is rough on a scale comparable to the escape depth for secondary electron emission (5–15 nm), we might also expect that E_2 would almost be independent of the angle of beam incidence. Butler *et al.*[16] have observed that some processed polymer surfaces do indeed have a flat E_2 vs. tilt variation. Thus an E_2 profile may be a useful tool for the characterization of such microtextured polymer surfaces.

ADVANTAGES

Compositional vs. topographical contrast

Until now we have been chiefly concerned with obtaining and understanding secondary electron image contrast produced as a result of differences in chemical composition within the sample. It should be emphasized that such ideas are relevant only within the context of low-voltage SEM, which can be operated within the realm of E_2 for most materials. Similarly none of the discussion is relevant in terms of conventional SEM, which is capable of producing only topographical contrast in secondary electron imaging mode. Unfortunately the converse situation, LVSEM in which there is no topographical contrast, never exists; in the final image there is always some degree of topographical contrast superimposed on the compositional contrast, and topography often dominates.

It would then appear that, by ignoring the effects of topographical contrast, we have oversimplified the

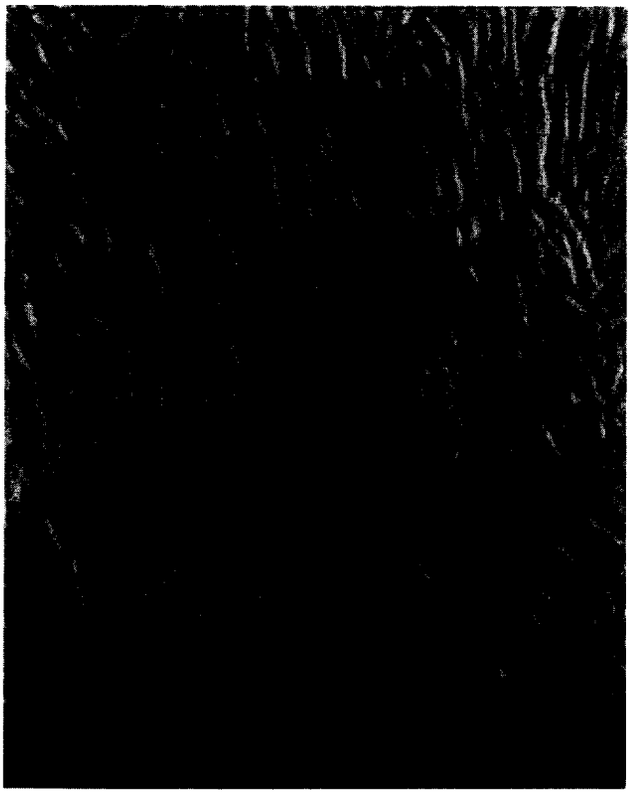

Figure 10 Lamellar bundles in an uncoated, unstained and unsectioned biaxially oriented polyethylene (PE) film surface

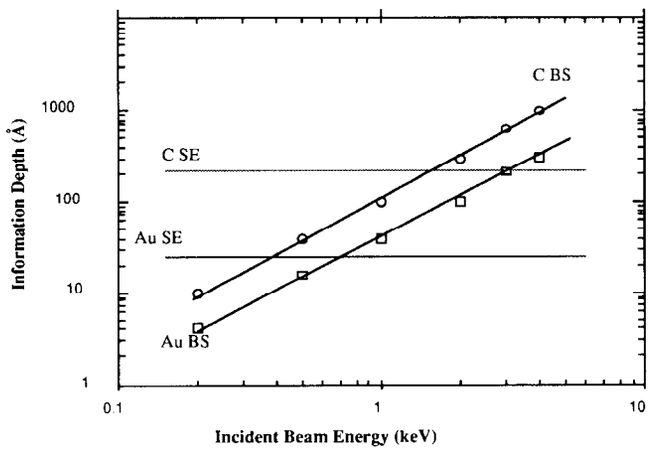

Figure 11 Variation of information depth in backscatter (BS) and secondary electron (SE) image modes in carbon and gold as a function of incident beam energy

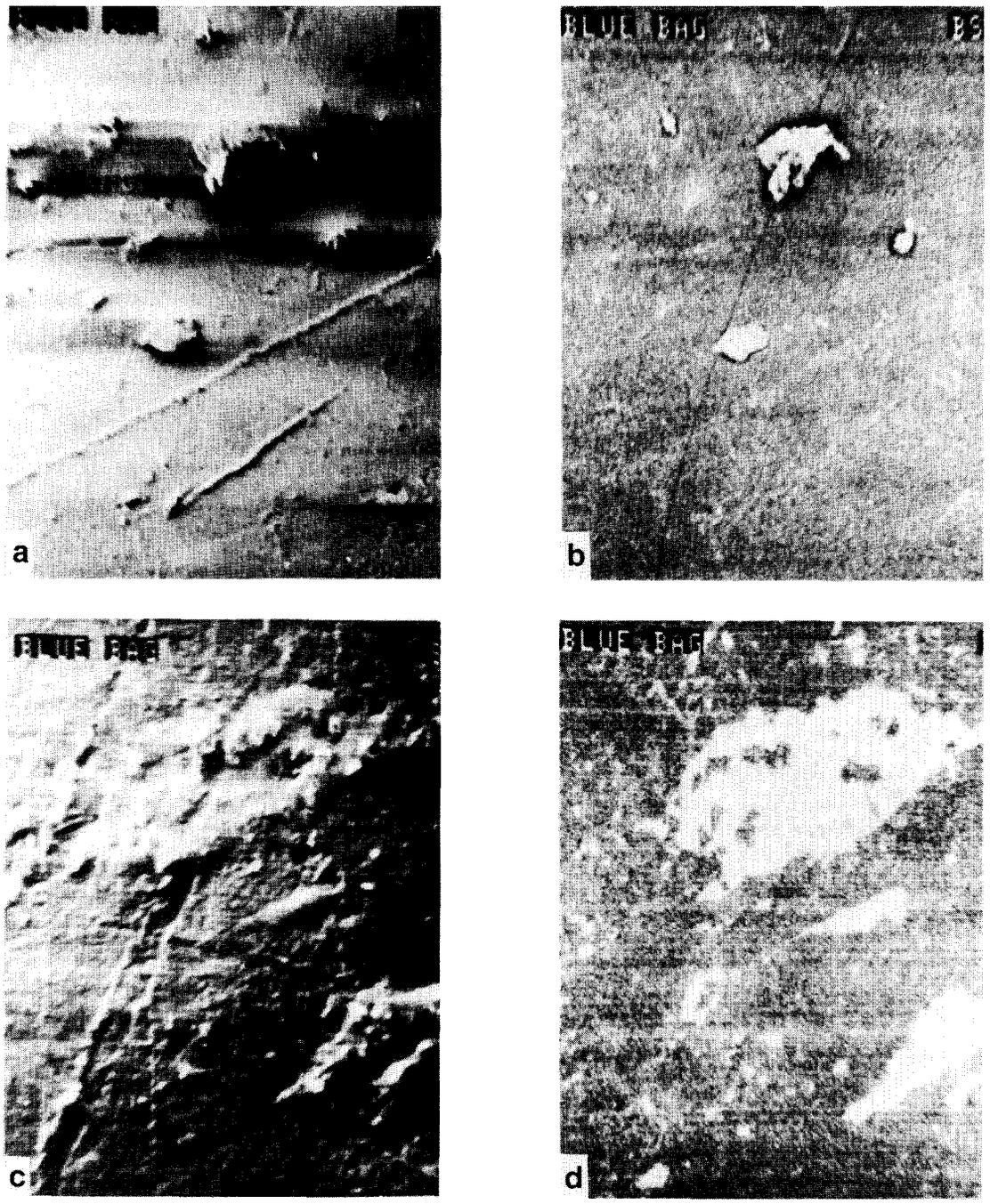

Figure 12 Comparison of SE vs. BS imaging of polymer film in the LVSEM. (a) and (b) Comparison of the same area at low magnification in the SE and BS modes. The stability and lack of charging in the BS image is evident. (c) and (d) A similar comparison to (a) and (b) but demonstrating how much extra information the combination of SE and BS modes gives. Notice the two shades of white, indicating at least two high-Z components

situation; and for the purpose of secondary electron imaging, this is indeed true. However, the high topographical resolution attainable in the LVSEM can be advantageous in its own right.

Structure–properties investigations

The physical properties of any polyolefin product are ultimately determined by the relative degree and arrangement of the amorphous and crystalline fractions. One way to assess the microcrystalline morphology is to observe directly the crystalline lamellar bundles: their relationship to each other and to the amorphous phase. Conventionally this is done with TEM, using any of several heavy-metal staining or chemical extraction methods of specimen preparation[17–19], but the nature of these experiments is frequently not conducive to wide-scale experimentation. Often the interest is in the morphology of a finished product, which has been fabricated via some type of stress-induced crystallization. Experiments that involve such materials require TEM views along the three principal processing directions; in the case of injection-moulded parts, the angle of TEM viewing is determined by such parameters as knit lines and distance from injection gates. In any typical case the required sample preparation time alone can be prohibitive.

Lamellar imaging with the LVSEM is a simple and straightforward application of purely topographical contrast: *Figure 10* shows lamellar detail of an *uncoated, unstained* and *unsectioned* PE film surface. For a finished product study, the samples can be cut (faced instead of sectioned) in the correct directions and directly examined in the LVSEM at a rate of several specimens per day.

Backscattered to the future

In the conventional SEM situation, backscattered electrons emerge from a deeper, more delocalized region than the secondaries and, consequently, have poorer resolution (cf. *Figure 1*). However, elastic scattering events are more localized than inelastic phenomena, and thus backscattered images always improve in resolution as E_0 decreases. As can be seen from *Figure 11*, at energies below about 1.5 keV the BS depth of information becomes comparable to, and ultimately less than, the SE value. Thus it will be BS images that will carry the most useful surface detail at low incident beam energies.

Also, the intensity of BS emission is directly proportional to the specimen atomic number, Z; thus the contrast obtained in BS images is strongly compositional in origin. Unfortunately, the decrease in BS emission as a function of accelerating voltage (coupled with the low $Z = 12$ for C) brings the BS signal intensity for polymeric materials below the detectable level of conventional BS detectors. Thus the high resolution that is theoretically attainable in BS images has not been demonstrated.

However, there is a new type of BS detector based on microchannel plate technology that is sensitive to slight variations in very low BS signal intensities[5]. An example of their performance is offered in *Figure 12*. These BS images of a generic (i.e. store-bought) garbage bag clearly show differing shades of grey, which correspond to compositional differences.

ACKNOWLEDGEMENTS

We are indebted to Exxon Chemical Company for their support of our research programme. We are equally grateful to Hitachi Scientific Instruments for their loan of the equipment on which some of this work was performed.

REFERENCES

1 Joy, D. C. *J. Microsc.* 1985, **140**(3), 283
2 Pawley, J. B. *J. Microsc.* 1984, **136**(1), 45
3 Berry, V. K. *Scanning* 1988, **10**, 19
4 Postek, M. T., Keery, W. J. and Larrabee, R. D. *Scanning* 1989, **11**, 111
5 Postek, M. T., Keery, W. J. and Frederick, N. *Rev. Sci. Instrum.* 1990, **61**(6), 1648
6 Seiler, H. 'Electron Beam Interactions with Solids', Proc. 1st Pfefferkorn Conf., Monterey, CA (Eds D. F. Kyser, H. Niedrig, D. E. Newbury and R. Shimizu), Scanning Electron Microscopy Inc., AMF O'Hare, IL, 1982, p. 34
7 Gross, B., von Seggern, H. and Berraissoul, A. *IEEE Trans. Electr. Insul.* 1987, **EI-22**(1), 23
8 Vaz, O. W. and Krause, S. J. Proc. 44th Ann. Mtg Electron Microsc. Soc. Am. (Ed. G. W. Bailey), San Francisco Press, San Francisco, CA, 1986, p. 676
9 Salow, H. *Phys. Z.* 1940, **41**, 434
10 Bethe, H. *Phys. Rev.* 1941, **59**, 940
11 Dekker, A. J. *Solid State Phys.* 1958, **6**, 251
12 Burke, E. A. *IEEE Trans. Nucl. Sci.* 1980, **NS-27**, 1760
13 Kishimoto, Y., Oshima, T., Hashimoto, M. and Hayashi, T. *J. Appl. Polym. Sci.* 1990, **39**, 2055
14 Joy, D. C. *J. Microsc.* 1987, **147**, 51
15 Sugiyama, N., Ikeda, S. and Uchikawa, Y. *J. Electron Microsc.* 1986, **35**, 9
16 Butler, J. H., Joy, D. C., Bradley, G. F., Krause, S. J. and Brown, G. M. *Microscopy: The Key Research Tool* 1992, p. 103
17 Sano, H., Usami, T. and Nakagawa, H. *Polymer* 1986, **27**, 1497
18 Voight-Martin, I. G., Fischer, E. W. and Mandelkern, L. *J. Polym. Sci., Polym. Phys. Edn.* 1980, **18**, 2347
19 Sawyer, L. C. and Grubb, D. T. 'Polymer Microscopy', Chapman & Hall, New York, 1987